Supplementary Information Report Number 1

12km Dynamical Downscaling Documentation

Authors: Simon Tucker[1], Chang Wang[1], Richard Jones[1], Grace Redmond[1], Erasmo Buonomo[1], Stuart Webster[1]

Met Office internal reviewers: Gill Martin[1], David Hein[1]

1 - Met Office, Exeter, UK

Contents

S1.1 Introduction

This report provides documentation of the downscaling experiments performed in the Second National Climate Change Study and of the model output data that has been delivered in product 3.1. The report is intended to enable easy access and understanding of the datasets provided, and includes details of:

- HadGEM3-RA model configuration
- Regional domain
- Time periods and scenarios
- Description of GCMs / Aspects of RCM configuration specific to the driving GCM
- Model inputs
- Model diagnostic outputs

In the dynamical downscaling work, nine GCMs from the CMIP5 archive (see http://cmip-pcmdi.llnl.gov/cmip5/) were downscaled along with the ERA-Interim reanalysis over a domain covering Southeast Asia. The selection of the downscaled GCMs is described in Chapter 3; the models selected are ACCESS1-3, BCC-CSM1-1-m, CMCC-CM, CNRM-CM5, CSIRO-Mk3-6-0, CanESM2, GFDL-CM3, HadGEM2-ES and IPSL-CM5A-MR. Originally a tenth GCM, GFDL-ESM2G, was also going to be downscaled. The reasons for not using this GCM are discussed in the Chapter 4.

S1.2 HadGEM3-RA model configuration

HadGEM3-RA is a regional climate model (RCM) that uses the third global atmosphere (GA3) configuration (a defined set of science settings) of the Met Office Unified Model (hereafter referred to as the UM). A description of the HadGEM3-RA model, along with an evaluation over Africa is given in Moufouma-Okia and Jones (2014). For a full description of the GA3 formulation, refer to Walters et al. (2011).

The model used in this project differs from the standard HadGEM3-RA model in the following ways:

1. HadGEM3-RA in its standard configuration has 63 vertical levels and a top atmospheric height of 40km. Many of the global models downscaled have lower top heights. For these models, levels have been removed from the top of the RCM as required. The performance of parameterisation schemes in the troposphere is sensitive to the vertical resolution; in view of this all GA3 configurations have a common first 50 levels which model the first 18km of the atmosphere. By keeping the same first 50 levels (and keeping higher levels in common where possible) there is partial consistence with the GA3 configuration. Section 5 gives details of what level set was used for each GCM.
2. Additional smoothing to the resolved and parameterised orography has been applied in order to keep the model numerically stable. The requirement for smoothing the orography in the UM and the method used are described in Webster et al. (2003). The smoothing in these experiments has used ε=30, where ε has the same meaning as in equation one of Webster et al. (2003). This level of smoothing is used in 12 km limited area UM simulations over Southeast Asia. It means that the grid-scale orographic features are eliminated completely, 6 grid-length features are damped by 50% and 10 grid-length (and longer) features remain largely untouched. Calculation of the standard deviation fields that are used in the gravity

wave drag parameterisation scheme is performed relative to the filtered mean orography. Consequently, information lost from the resolved orography by the filtering process has been added to the fields used in some of the model's parameterisation schemes. Smoothing of the standard deviation fields has been performed in the same way as that of the mean orography.

3. A limit (referred to as the w limiter) on the maximum vertical motions was applied at model level 26 (approximately 5km) and above. The limit applied was a vertical Courant number of 1.5. At model level 26 this roughly translates as a limit of 2.9 m/s, with this limit increasing as level thickness increases. The limit was chosen to only be activated where the resolved vertical motions became unrealistic and was implemented to avoid occasional model crashes. The number of times the limiter was applied was carefully monitored.
4. In order to keep the model stable without over-relying on the w limiter, a 3 minute time step (rather than 5 minute) was used. The time step is the discrete length of time that the model integrates forward by. A shorter time step ensures a more accurate integration at the expense of making the simulation more computationally expensive.

S1.3. Regional domain, model resolution and land sea mask

The RCM experiments were run over a domain (Figure S1.1) covering 94° to 126.89° longitude and -11.1° to 20.69° latitude. The grid box spacing is 0.11° *(equivalent to ~12 km at these latitudes)* meaning that there are 300 grid boxes in the East-West direction and 290 grid boxes in the North-South direction.

When choosing domains and resolutions, the affordability of simulations needed to be considered. There was a need for balance between the affordability of a single simulation and the number of GCMs and scenarios to downscale.

A high resolution was desired in order to resolve Singapore adequately. The chosen resolution was considered the highest possible resolution for which the single nesting methodology could be used with the majority of CMIP5 models. Further discussion on this subject is given in section 5. At the beginning of the project a number of domains were trialled. The trials involved one year long simulations driven by the ERA-Interim reanalysis. Comparisons were then made of the following:

- The 950 hPa winds. Consistency with the driving reanalysis data was assessed during two monsoon seasons (approximated as DJF and JJA).
- The diurnal cycle of rainfall over Singapore was compared as a test of the dependence on the domain size and positioning on the RCM's production of local processes. Hourly rainfall is not expected to be reproduced correctly at 12km resolution, however this test is still relevant since 1) Singapore is located in the middle of the domain, where the RCM is less constrained by the large scale flow (Jones et al., 1995) and 2) rainfall in Singapore is mostly the outcome of mesoscale processes which can be attributed to the RCM only, since they are not explicitly resolved at GCM scale.

There were three domains where the level of consistency was sufficient and also produced very similar diurnal cycles over Singapore. Consequently, these three domains were considered suitable from a scientific point of view. The final choice was made in consultation with MSS.

The land-sea mask is shown in Figure S1.1. The positioning of the grid was designed to ensure that Singapore was represented by as many grid boxes as possible. In addition the number of land points for Singapore was increased to take into account recent land reclamation projects which are not represented in the dataset used to derive the land-sea mask. Careful consideration was given to the land sea mask of the whole domain in order to ensure that it was accurate.

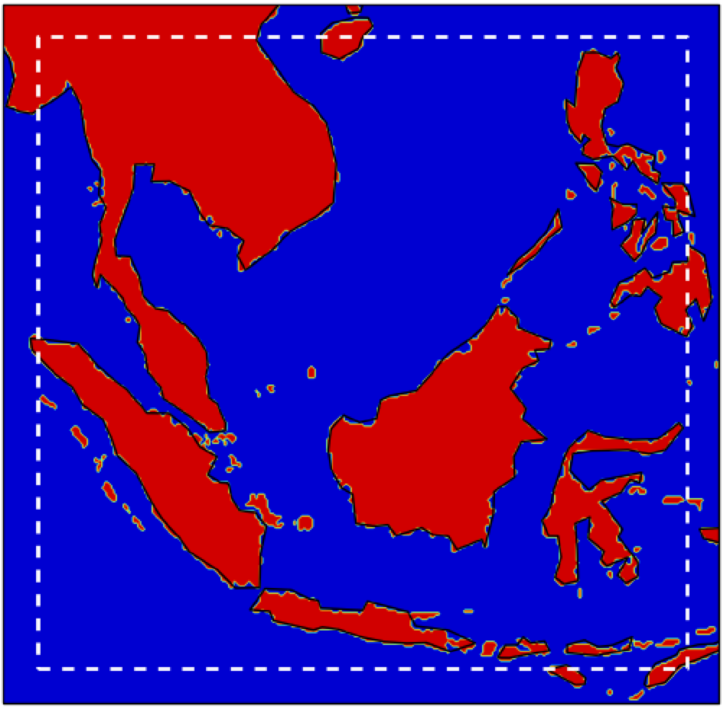

Figure S1.1: Plot of the land sea mask. Red represents land, blue represents ocean. The white line marks the boundary between the outer 'rim region' (as described in section S1.6.1) and the interior of the RCM domain.

S1.4 Time periods and scenarios

The simulations covered the historical period and used two scenarios: RCP45 and RCP85. The scenarios are part of four future plausible trajectories of different aspects of the future that were constructed to investigate the potential consequences of anthropogenic climate change in CMIP5, referred to as "Representative Concentration Pathways" or RCPs (Moss et al., 2010). These future scenarios have been generated by Integrated Assessment Models that combine socio-economic and energy-system modelling to produce plausible future estimates of factors that affect the climate, specifically greenhouse gas concentrations, aerosol, tropospheric ozone and land use. These factors are often described as climate forcings. For more information about the RCP and historical forcings used in CMIP5 and how they are applied in these simulations, see section S1.6d.

The CMIP5 GCMs forked into RCP scenarios in 2006. In order to allow more observations to be used for evaluation and bias adjustments, it was desirable to have a historical period that extended closer to the present day. The historical period was extended to 2009 by using RCP85 model inputs and forcings. Any error from using the first four years of RCP85 greenhouse gas concentrations, aerosol, ozone and land use rather that observed is expected to be insignificant.

The RCM Scenario simulations span the period 1/11/2009 - 1/12/2099. An obvious consequence of this set up is that there will be no continuation of weather systems between the last day of the historical RCM simulation and the first day of the RCP45 RCM simulations.

In order to the run the experiments and produce data in a timely fashion, the simulations have been split into periods of typically thirty years. This enabled experiments to be run in parallel and also the prioritisation of time periods that are analysed in reports. Table S1.1 shows the start and finish years of each segment.

At the start of each simulation, the RCM solution will be influenced by its initial conditions. Consequently, the first eleven months of each simulation have been discarded as spin-up. See section S1.6c for more information on the initialisation of each simulation and justification of the spin-up period.

Table S1.1:

Start date	Start of analysed data	End date	Comments
1/12/1950	1/11/1951	1/12/1959	
1/12/1958	1/11/1959	1/12/2009	Switch to RCP85 scenario forcings on 1/12/2005
1/12/2008	1/11/2009	1/12/2039	For both scenarios
1/12/2038	1/11/2039	1/12/2069	For both scenarios
1/12/2068	1/11/2069	1/12/2099	For both scenarios. Exceptions in table 1A

It was necessary to further split some simulations. These are detailed in table S1.1A.

Table S1.1A:

Start date	Start of analysed data	End date	GCM and scenario
1/12/2068	1/11/2069	1/12/2093	CNRM-CM5 RCP85
1/12/2092	1/11/2093	1/12/2099	CNRM-CM5 RCP85
1/12/2068	1/11/2069	1/12/2076	CNRM-CM5 RCP45
1/12/2075	1/11/2076	1/12/2084	CNRM-CM5 RCP45
1/12/2083	1/11/2084	1/12/2091	CNRM-CM5 RCP45
1/12/2090	1/11/2091	1/12/2099	CNRM-CM5 RCP45
1/12/2068	1/11/2069	1/6/2093	ACCESS1.3 RCP85
1/12/2092	1/6/2093	1/12/2099	ACCESS1.3 RCP85

Although two spun-up RCM simulations covering an overlapping time period would be expected to be climatologically similar, the solutions would not be expected at a specific time to necessarily be the same. The range of solutions to RCM simulations that only differ in the initial conditions is a consequence of the internal variability of the RCM and has been the subject of numerous studies (e.g. Caya and Biner, 2004). For convenience we have joined simulations on the 1st of November in all cases; however, users requiring continuous time series may wish to find a date where there is lower internal variability to join simulations.

S1.5. Description of driving GCMs, Aspects of RCM configuration specific to driving GCM

Nine GCMs from the CMIP5 archive were downscaled along with the ERA-Interim reanalysis. Each GCM will have its own dynamical core with differing prognostic variables, coordinate systems and resolutions. Table S1.2 describes some of the properties of each model with links or references to more information. Note that CMIP5 conventions specify a standard set of model variables to be output. Most modelling centres have chosen to output data on a standard horizontal grid, consequently information on the GCM's native horizontal coordinates or prognostic variables have not been included; interested readers may refer to the links in Table S1.2. During the downscaling, the GCMs provide the RCM with input atmospheric lateral boundary conditions (LBCs) and sea surface temperatures (SSTs). More information on the preparation of RCM input data is given in section S1.6.

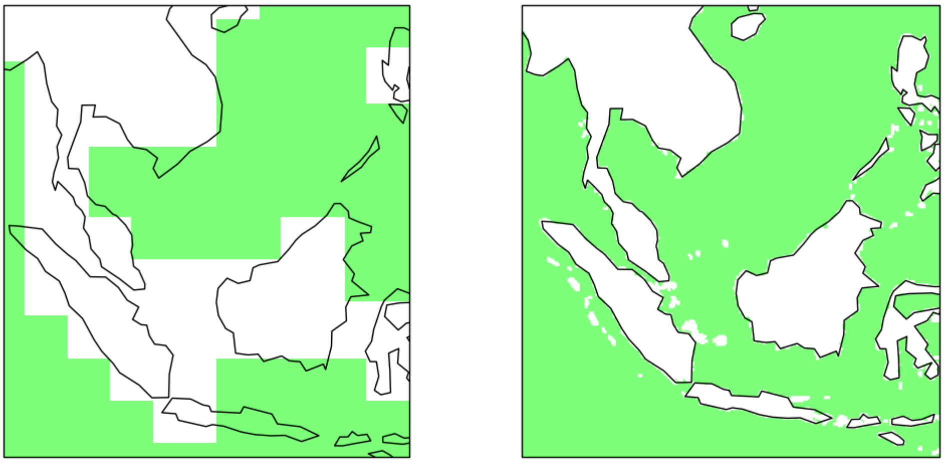

Figure S1.2: (Left) the land sea mask of the CanESM2 GCM over the RCM domain at its native resolution. (Right) the RCM domain at its resolution (12km). In both plots white represents land and green represents ocean. It should be noted that the CanESM2 GCM has been selected to plot since it contains the largest differences.

The 'Big Brother' experiments (Denis et al, 2002) involved performing a high (at the time) resolution 'reference' climate simulation, before applying a statistical filter in order to reduce the resolution of the output. The filtered data was then used in order to drive an RCM in a series of experiments designed to test different aspects of one-way nesting set up, by accessing the reproducibility of the climate of the reference simulation. One such experiment (Denis et al., 2003), assessed the sensitivity of resolution jump between the RCM and driving data. They found that a resolution jump of 12 was able to satisfactory reproduce the climate of the reference simulation, whilst a jump of 24 was not. The Big Brother experiments were performed over Canada and it is unclear how applicable the conclusions are for other regions, particularly for Southeast Asia where the large scale atmospheric flow is weaker but the influence of sea surface temperatures on the atmosphere is greater.

The change in resolution also means that the land sea masks of the GCM (over the RCM domain) and RCM can differ significantly, as illustrated in Figure S1.2, where large parts of the domain have switched from land to ocean. A consequence of this is that SSTs have to be extrapolated on to the RCM domain, and hence high resolution details being lost, e.g. SSTs tending to be warmer in the Strait of Malacca. More details on the interpolation procedure of SSTs are provided in section 6b. It is also possible that such a significant change from land in the GCM to ocean in the RCM will cause the hydrological balance of the two models to differ, leading to inconsistencies between the two simulations. It is likely that the SSTs and lateral boundary conditions provided to the RCM will contain both model bias and a resolution jump. In view of the above discussion, the information in table S1.2 and the analysis of the GCMs given in the Chapter 3 provide useful information that aids interpretation of the RCM outputs.

Many climate models use simplified calendars, such as the 360 day calendar (where every month has 30 days) and the 365 day calendar (where there are no leap years). The RCM simulations use the same calendar as the driving GCM. The calendar used in the GCM is given in Table S1.2. Table S1.2 also contains the number of levels used in the RCM (see section s1.1 on RCM formulation for more explanation).

Table S1.2:

Component	Atmosphere				Ocean			
GCM	Approx. Horiz. grid spacing in tropics (long., lat. spacing)	Vert.l grid type *	No. of vertical levels	Top height	Approx. Horiz. grid spacing in tropics (long., lat. spacing)	Calendar	Links or references	No. of levels in RCM
ACCESS1-3	1.9,1.2	HH	38	39000m (36000m for winds)	1.00,0.34	Gregorian	http://wiki.csiro.au/confluence/display/ACCESS/ACCESS+Publications	63**
BCC-CSM1-1-m	1.1,1.1	HP	26	354Pa	1.00,0.34	365 day	Wu et al., 2014	59
CanESM2	2.8,2.8	HP	35	102Pa	1.40,0.93	365 day	http://www.cccma.ec.gc.ca/models	62
CMCC-CM	0.8,0.80	HP	31	1000Pa	2.00,0.50	Gregorian	http://www.cmcc.it/data-models/models	58
CNRM-CM5	1.4,1.4	HP	31	1000Pa	1.00,0.33	Gregorian	http://www.cnrm.meteo.fr/cmip5 Follow model description link	58
CSIRO-Mk3-6-0	1.9,1.9	HP	18	446Pa	1.88,1.88	365 day	Rotstayn et al., 2010	59
GFDL-CM3	2.5,2.0	HP	48	2Pa	1.00,0.34	365 day	http://nomads.gfdl.noaa.gov- follow links	62
HadGEM2-ES	1.9,1.2	HH	38	39000m(36000m for winds)	1.00,0.34	360 day	The HadGEM2 Development Team, 2011 Collins et al. ,2011	63
IPSL-CM5A-MR	2.5,1.3	HP	39	4Pa	2.00,0.50	365 day	http://icmc.ipsl.fr	63
ERA-INTERIM	0.8,0.8	HP	64	10Pa	0.25,0.25 switching to 0.05,0.05***	Gregorian	Dee et al., 2011	64

***Here "HH" stands for hybrid height, and "HP" stands for hybrid pressure. Appendix S1.2 gives a brief description of both coordinate systems.

****** The level set used here is slightly different: Instead of removing a level from the top, the 63 levels have been rescaled. Comparison with the standard L63 GA3 level set shows that they are coincident up to approximately 7km and then only differ by a tiny amount thereafter, such that even by the time 20km is reached, the location of the model level is approximately only 1/4 of the level thickness at that height (and thus the RCM's physical configuration should be preserved). The slightly different approach is not due to a deliberate experimental design decision.

******* SSTs used in RCM simulation come from high resolution SST reanalysis that combine observations and satellite data: see section S1.6B for more information.

S1.6. Model Inputs

S1.6.1 Lateral boundary conditions

Information from the driving GCM is passed to the RCM at the lateral boundaries of the RCM domain incrementally as the regional model integrates forward in time.

CMIP5 GCM data are stored in an archive which contains the following variables output at a six hourly instantaneous frequency: (three dimensional) westerly/northerly winds, temperature, specific humidity and (two dimensional) surface pressure. During the creation of lateral boundary conditions, there is a requirement for UM prognostic variables to be derived, along with vertical and horizontal interpolation on to the boundaries of the RCM grid. The procedure used to create lateral boundary conditions is outlined in Appendix S1.2.

The RCM solution in the outermost four grid points comes entirely from the driving model and is required for the RCM's semi-Lagrangian dynamical core. After that a gradual relaxation from the GCM to RCM atmospheric conditions is applied over four grid points where the GCM forms 1, 3/4,1/2,1/4 of the solution. Over the area where lateral boundary conditions are applied the RCM uses orography from the driving GCM (that has been bi-linearly interpolated on to the RCM grid), the next seven most outer points contain a blending between the RCM and GCM orography. For this reason data from the 15 most outer grid points is often not suitable for analysis and is excluded. This 15 point 'rim region' is marked with a white line in Figure S1.1.

Lateral boundary conditions are supplied at every RCM time step by incrementally linearly interpolating in time from the current model time provided by the incoming six-hourly instantaneous data value to the next six-hourly value.

One feature of the implementation of the downscaling of the IPSL-CM5A-MR model is that three hours have been subtracted from the true time of the data in order to change the data times from 3,9,15, and 21 hours to the more conventional 0,6,12 and 18 hours used in the other CMIP5 driving GCMs. Tests in a one year simulation using correct LBC times show that the consequences of this are minimal.

S1.6.2 Sea Surface Temperatures

Daily mean sea surface temperature (SST), taken from the ocean component of the driving GCM, was provided as input to the regional model. Note that the CMIP5 archive provides SST output on both the atmosphere and ocean grid. Data from the ocean grid has been used as this tends to be higher resolution. The SSTs were prepared for input by using the following procedure:

- SSTs on the source model grid were first interpolated onto land points of the source model grid. This was done to ensure that information was not lost around the coasts in the interpolation process as well as avoiding any possible mis-matches between the GCM and RCM land masks.
- The CMIP5 models to be downscaled use a variety of ocean grids. The land-filled data were then regridded using bilinear interpolation onto a common global regular latitude longitude grid. The resolution of the common grid was

chosen to match that of the highest model resolution over the tropics of the nine downscaled GCMs, namely a latitudinal resolution of *1/3°* and a longitudinal resolution of *1°*.

- Finally, the data were re-gridded using bilinear interpolation onto the 12km regional model domain ready to be input into the model.

For downscaling ERA-INTERIM, the model used daily high resolution reanalysis of SSTs that are a synthesis of satellite and in-situ observations. Unfortunately, there wasn't one product that covered the whole time period of the ERA-INTERIM reanalysis. The decision was therefore taken to use:

- Reynolds SSTs (Reynolds et al., 2007) for the period 1/12/1982-1/12/2008. This dataset is a 1/4° spatial resolution from November 1981 to 2008.
- OSTIA SSTs (Donlon et al., 2012 and Roberts-Jones et al., 2012) for the period 2008-2010. This dataset has a native resolution of 1/20° and covers 1985 to the present day.

With both Reynolds and OSTIA datasets, the SSTs on the source grid were first interpolated onto land points using the same method as used for the GCMs. Prior to being regridded onto the RCM domain, OSTIA SSTs were first regridded onto a 0.1° global grid by taking the average of the four source 0.05° grid boxes contained in each 0.1° grid box to make the OSTIA resolution roughly comparable to the RCM resolution. Figure S1.3 shows a comparison of Reynolds and OSTIA SSTs for the year 2008.

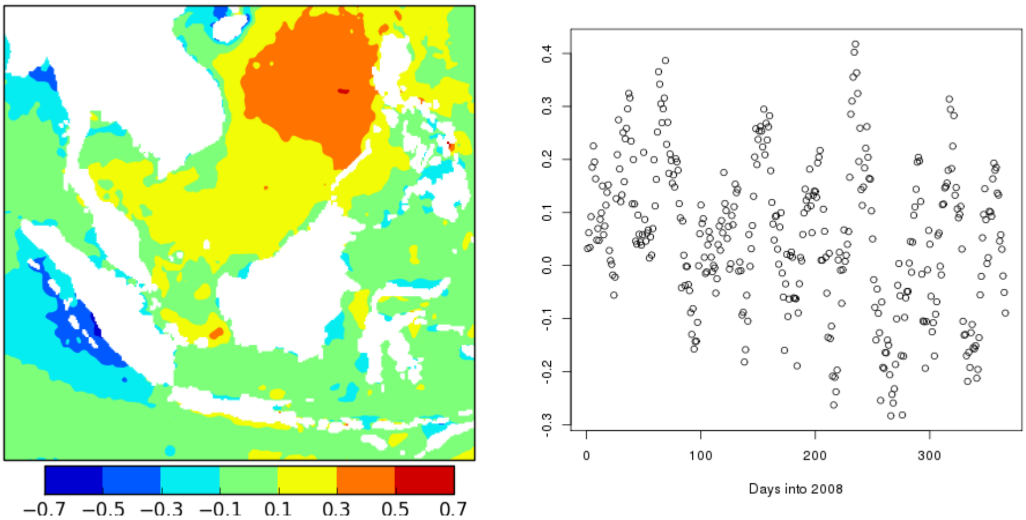

Figure S1.3: Differences between OSTIA and Reynolds SSTs (OSTIA-Reynolds) for the year 2008, after being regridded on to the RCM domain. Left: annual mean. Right: domain averaged daily time series.

S1.6.3 Initial conditions

The model was initialised with atmospheric conditions and sea surface temperatures coming from the driving GCM. These variables need to be initialised to avoid model instabilities at the start of the simulation due to disagreement between initial conditions and lateral boundary conditions.

At the start of each simulation, the RCM solution will be influenced by its initial conditions. Consequently it is necessary to allow the atmosphere and land surface to adjust or "spin-up" to a mutual equilibrium state. Soil moisture and temperature can take many months to reach equilibrium due to the thermodynamic processes that control them. As soil moisture and temperature modulate surface latent and sensible heat fluxes, it is likely that the RCM's climate will drift (when measured as a deviation from the driving GCM) during this period. Ideally, soil moisture at all levels will be spun up, however it is the soil moisture in the root zone that has the most influence on the climate. For a discussion on this topic see Giorgi and Mearns (1999).

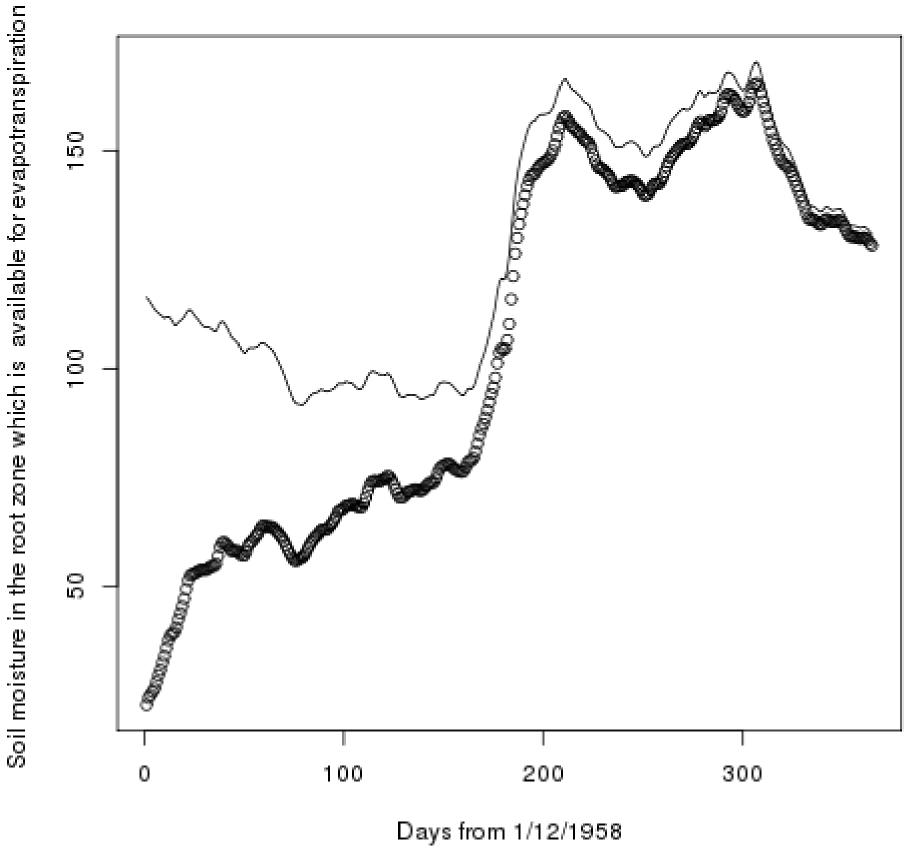

Figure S1.4: Plot shows a time series of domain averaged soil moisture in the root zone that is available for evapotranspiration. The dots are for a simulation that was initialised on 1/12/1958 and the lines are from a spun up (began in 1950) simulation that is otherwise identical. The two simulations have similar values after 350 days, indicating that the simulations have spun up. The driving GCM in this plot is CSIRO-Mk3-6-0; plots with other driving GCMs look similar.

In order to reduce the length of required spin-up, it may be desirable to initialise soil variables from the driving GCM. Unfortunately this is only possible for HadGEM2-ES, since the land models used in other GCMs will not share the same soil levels. Non Hadley Centre GCMs have soil variables initialised from HadGEM2-ES and it is hoped that these values will be roughly sensible. An eleven month spin-up period has been chosen based on Figure S1.4.

S1.6.4 RCP forcing data

Forcing data can be retrieved from the CMIP5 forcing data webpage: http://cmip-pcmdi.llnl.gov/cmip5/forcing.html. The remaining subsections describe how each dataset was applied in these simulations.

S1.6.4.1 Land use

A 0.5° gridded dataset of land use was provided as part of the forcing data to be used in CMIP5 models that do not contain a dynamic vegetation model (Hurtt et al., 2011). This dataset contains fractions of the following land use types: crop, pasture, water/ice, urban and natural (split into primary and secondary).

In the RCM, vegetation-atmosphere interactions are calculated using the Joint UK Land Environment Simulator (JULES, Best et al., 2011). JULES splits each RCM grid box into 9 ‘tiles’ that include 5 types of vegetation (broadleaf trees, needleleaf trees, C3 grass, C4 grass and shrubs) and 4 other types (urban, water, soil and ice).

In order that the CMIP5 land use forcings can be used in the RCM, it is necessary to find a method for mapping between these land use fractions and the JULES tiles. Mapping between land use and land cover is not straightforward. Methods typically involve using a potential vegetation dataset and a set of rules to define transitions for other data types. Fortunately, the ISAM-HYDE dataset (Meiyappan et al., 2011) is a 0.5° land cover dataset consistent with the HYDE3.1 land use dataset (the source for the historical period of CMIP5 land use forcing) and is also in agreement with satellite observations of the present day. We have taken the ISAM-HYDE dataset and mapped their land cover types to JULES tiles. The mapping used is provided in Appendix S1.1. For the scenarios, the following assumptions have been made in converting from land use to land cover types:

- The ratio of all natural land types (i.e. broad-leaved tree, needle-leaved trees, natural grass, shrub and bare-ground) remains fixed with respect to the total fraction of natural land. This ratio has been calculated from the 2004 ISAM-HYDE land cover dataset. What varies is the total fraction of land that has natural (both primary and secondary) use.
- The C3:C4 grass ratios do not change from the year 2005.

The data are mapped from the global to the RCM grid using nearest neighbour interpolation. This interpolation method rather than bilinear interpolation has been chosen in order to not further smooth the data and hence enhance the resolution mis-match. The Singapore grid boxes are represented by a combination three of the nine JULES tiles, namely: broadleaf tree (referred to as ‘forest’ in figure S1.5), C3 grass and urban. Figure S1.5 shows the resulting land cover over Singapore for the historical period. Land cover over Singapore does not change in either the RCP45 or RCP85 scenario.

It should be noted that this land use mapping and the resulting land cover in the RCM will not necessarily be the same as that applied in the driving GCMs, even those which did not include a dynamic vegetation model.

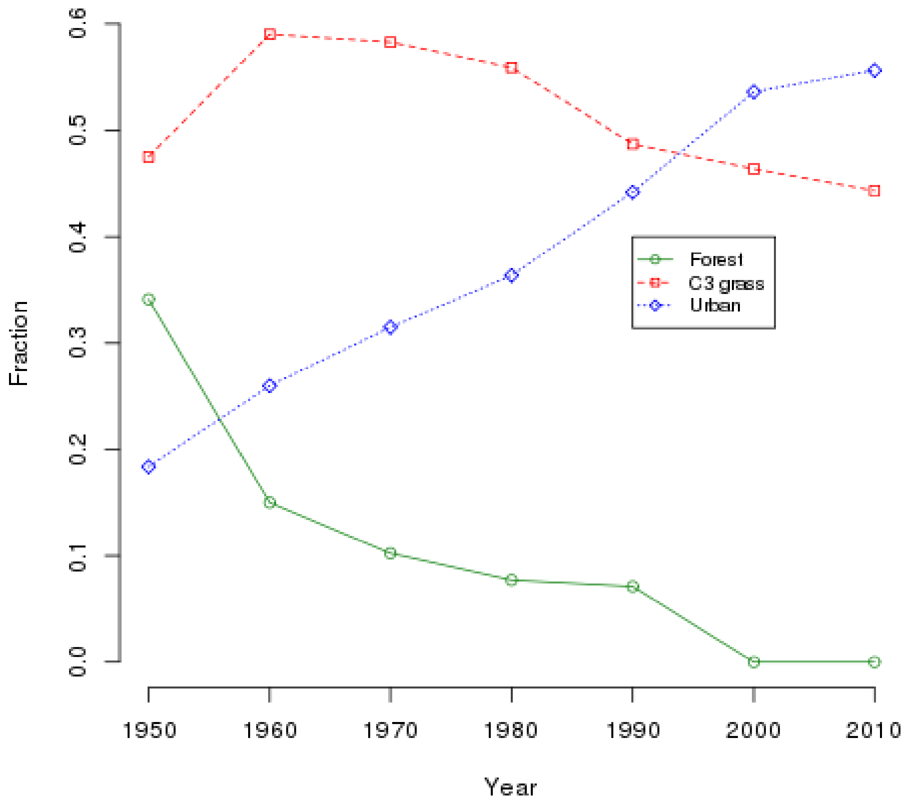

Figure S1.5: Land cover fractions over Singapore following the mapping of the ISAM-HYDE dataset on to JULES tiles. "Forest" refers to broadleaf tree.

S1.6.4.2. Greenhouse Gas Concentrations

The CO2, CH4, N2O and Halocarbons were supplied from the CMIP5 data portal as global mean mass mixing ratios. The annual concentrations were interpolated linearly at each RCM time step.

S1.6.4.3. Ozone

Ozone has come from the AC&C/SPARC ozone database (Cionni et al., 2011) which covers the period 1850 to 2100. CMIP5 models that do not include a chemistry model also use this dataset. Zonal means have been calculated from this dataset by averaging all the values that are at a constant latitude, and the data has been interpolated on to the height based UM grid using the method described in section 4.2 of Jones et al.(2011).

S1.6.5. Aerosols

HadGEM3-RA does not interactively model aerosols, however aerosol climatologies are used to provide aerosol concentrations to the RCM (for use in parameterisations that require aerosol values). The climatologies are three dimensional and also include an annual cycle by providing data for each month of the year. The climatologies are calculated from an atmosphere-only HadGEM2 experiment with added earth system components.

Table S1.3

		MONTHLY	DAILY			6 HOURLY	3 HOURLY		1 HOURLY
cf variable name	**Met Office variable name**	**Mean**	**Max**	**Mean**	**Min**	**Inst**	**Inst**	**Mean**	**Mean**
air pressure at sea level	PRESSURE AT MEAN SEA LEVEL	E,P		E					
air temperature at 1.5m	TEMPERATURE AT 1.5M	DP,E,P	DP,E,P	DP,E,P	DP,E,P		E		
air temperature on pressure levels	TEMPERATURE ON P LEV/UV GRID			E,P					
cloud area fraction	TOTAL CLOUD AMOUNT IN LW RADIATION	E.P							
Convective rainfall rate	CONVECTIVE RAINFALL RATE	E		E				E	
eastward wind at 10m	10 METRE WIND U-COMP B GRID			E,P					
eastward wind on pressure levels	U COMPNT OF WIND ON P LEV/UV GRID	E,P		E,P					
Northward wind at 10m	10 METRE WIND V-COMP B GRID			E,P					
northward wind on pressure levels	V COMPNT OF WIND ON P LEV/UV GRID	E.P		E,P					
precipitation flux	TOTAL PRECIPITATION RATE	DP,E,P		DP,E,P				E	E
relative humidity at 1.5m	RELATIVE HUMIDITY AT 1.5M	DP,E,P		DP,E,P					
relative humidty on pressure levels	"RELATIVE HUMIDITY ON P LEV/UV GRID	E							
specific humidity at 1.5m	SPECIFIC HUMIDITY AT 1.5M	E,P		E,P			E		
specific humidity on pressure levels	SPECIFIC HUMIDITY ON P LEV/UV GRID	E,P		E,P		E			
stratiform rainfall rate	LARGE SCALE RAINFALL RAT	E		E					
surface downwelling shortwave flux in air	TOTAL DOWNWARD SURFACE SW FLUX	E,P							
surface temperature	SURFACE TEMPERATURE AFTER TIMESTEP	E,P							
surface upward latent heat flux	SURFACE LATENT HEAT FLUX	E,P							
Wind gust	WIND GUST		E,P						
wind speed at 10.0m	10 METRE WIND SPEED ON B GRID	DP,E,P	E,P	DP,E,P					

S1.7. Model diagnostic outputs

The model outputs a wide range of diagnostics in the Met Office's PP binary data format. In the dynamical downscaling work a wide range of variables have been evaluated. Projections have been analysed for a subset of these variables. In Chapter 5 – Climate Change Projections, temperature, relative humidity and precipitation flux have first been bias corrected, details of the method used can be found in the report. Data for the eight RCM grid boxes that cover Singapore have also been placed on a data portal in order to make it available to policy makers in Singapore. Variables that have been bias corrected in the projections report have also been bias corrected before placing on the portal.

Table S1.3 lists the variables that are:

- Analysed in Chapter 4: Model Evaluation (E)
- Analysed in Chapter 5: Climate Change Projections (P)
- Available on the data portal (DP)

References

Best, M. J., Pryor, M., Clark, D. B., Rooney, G. G., Essery, R .L H., Menard, C. B., Edwards, J. M., Hendry, M. A., Porson, A., Gedney, N., Mercado, L. M., Sitch, S., Blyth, E., Boucher, O., Cox, P. M., Grimmond, C. S. B., and Harding, R. J. (2011) The Joint UK Land Environment Simulator (JULES), model description – Part 1: Energy and water fluxes, *Geosci. Model Dev*., 4, 677–699, doi: 10.5194/gmd-4-677-2011.

Caya D and Biner S (2004) Internal variability of RCM simulations over an annual cycle. Climate dynamics Volume 22 issue 1

Cionni, I., Eyring, V., Lamarque, J. F., Randel, W. J., Stevenson,D. S., Wu, F., Bodeker, G. E., Shepherd, T. G., Shindell, D. T., and Waugh, D. W. (2011): Ozone database in support of CMIP5 simulations: results and corresponding radiative forcing, Atmos. Chem.Phys. Discuss., 11, 10875–10933, doi:10.5194/acpd-11-10875-2011.

Collins, W.J., N. Bellouin, M. Doutriaux-Boucher, N. Gedney, P. Halloran, T. Hinton, J. Hughes, C. D. Jones, M. Joshi, S. Liddicoat, G. Martin, F. O'Connor, J. Rae, C. Senior, S. Sitch, I. Totterdell, A. Wiltshire, and S. Woodward. Development and evaluation of an Earth-System model: HadGEM2. Geosci. Model Dev., 4, 1051-1075, 2011.

Dee, D. P., Uppala, S. M., Simmons, A. J., Berrisford, P., Poli, P., Kobayashi, S., Andrae, U., Balmaseda, M. A., Balsamo, G., Bauer, P., Bechtold, P., Beljaars, A. C. M., van de Berg, L., Bidlot, J., Bormann, N., Delsol, C., Dragani, R., Fuentes, M., Geer, A. J., Haimberger, L., Healy, S. B., Hersbach, H., Hólm, E. V., Isaksen, L., Kållberg, P., Köhler, M., Matricardi, M., McNally, A. P., Monge-Sanz, B. M., Morcrette, J.-J., Park, B.-K., Peubey, C., de Rosnay, P., Tavolato, C., Thépaut, J.-N. and Vitart, F. (2011), The ERA-Interim reanalysis: configuration and performance of the data assimilation system. Q.J.R. Meteorol. Soc., 137: 553–597. doi: 10.1002/qj.828

Denis, B., Laprise, R., Caya, D. and Cote, J. Downscaling ability of one-way nested regional climate models: the Big-Brother experiment. (2002): Climate Dynamics 18: 627-648

Denis, B., Laprise, R. ad Caya, D. Sensitivity of a regional climate model to the resolution of the lateral boundary conditions. (2003):Climate Dynamics 20:107-126

Donlon, C. J., Martin, M., Stark, J., Roberts-Jones, J., Fiedler, E., and Wimmer, W (2012): The Operational Sea Surface Temperature and Sea Ice Analysis (OSTIA) system, Remote Sensing of

Environment, 116, 140 – 158, doi:10.1016/j.rse.2010.10.017, http://www.sciencedirect.com/science/article/pii/S0034425711002197, advanced Along Track Scanning Radiometer(AATSR) Special Issue.

Giorgi, F. and Mearns, L. Introduction to special section: Regional climate modelling revisited. (1999): Journal of geophysical Research, Vol104, No D6, Pages 6635-6352

G. C. Hurtt, L. P. Chini, S. Frolking, R. A. Betts, J. Feddema, G. Fischer, J. P. Fisk, K. Hibbard, R. A. Houghton, A. Janetos, C. D. Jones, G. Kindermann, T. Kinoshita, Kees Klein Goldewijk, K. Riahi, E. Shevliakova, S. Smith, E. Stehfest, A. Thomson, P. Thornton, D. P. van Vuuren, Y. P. Wang (2011) Harmonization of land-use scenarios for the period 1500â€“2100: 600 years of global gridded annual land-use transitions, wood harvest, and resulting secondary lands. Climatic Change 109:117â€“161 DOI 10.1007/s10584-011-0153-2

Jones, C. D., Hughes, J. K., Bellouin, N., Hardiman, S. C., Jones, G. S., Knight, J., Liddicoat, S., O'Connor, F. M., Andres, R. J., Bell, C., Boo, K.-O., Bozzo, A., Butchart, N., Cadule, P., Corbin, K. D., Doutriaux-Boucher, M., Friedlingstein, P., Gornall, J., Gray, L., Halloran, P. R., Hurtt, G., Ingram, W. J., Lamarque, J.-F., Law, R. M., Meinshausen, M., Osprey, S., Palin, E. J., Parsons Chini, L., Raddatz, T., Sanderson, M. G., Sellar, A. A., Schurer, A., Valdes, P., Wood, N., Woodward, S., Yoshioka, M., and Zerroukat, M.: The HadGEM2-ES implementation of CMIP5 centennial simulations (2011), Geosci. Model Dev., 4, 543-570, doi:10.5194/gmd-4-543-2011.

Jones,R., Murphy, J.M., and Noguer, M:Simulation of climate change over Europe using a nested regional climate model 1:Assessment of control climate, including sensitivity to location of lateral boundaries (1995), Q.J.R. Meteorol. Soc 121 pp pp 1413-1449

Meiyappan P. and Jain A.K.(2011) Three distinct global estimates of historical land cover and land-use conversions for over 200 years. Earth Sci. 6(2) pages 122-139

Moss, R. H., Edmonds, J. A., Hibbard, K. A., Manning, M. R.,Rose, S. K., van Vuuren, D. P., Carter, T. R., Emori, S., Kainuma,M., Kram, T., Meehl, G. A., Mitchell, J. F. B., Nakicenovic, N.,Riahi, K., Smith, S. J., Stouffer, R. J., Thomson, A. M., Weyant, J. P., and Wilbanks, T. J. (2010) The next generation of scenarios for climate change research and assessment, Nature, 463, 747–756

Moufouma-Okia. W. and R. G. Jones, (2014): Resolution dependence in simulating the African hydro-climate with the HadGEM3-RA Regional Climate Model (Climate Dynamics in press)

Reynolds, R. W., T. M. Smith, C. Liu, D. B. Chelton, K. S. Casey, and M. G. Schlax, 2007: Daily high-resolution blended analyses for sea surface temperature. J. Climate, 20, 5473-5496.

Roberts-Jones, J., Fiedler, E. K., and Martin, M. J.: Daily, Global, High-Resolution SST and Sea Ice Reanalysis for 1985-2007 Using the OSTIA System, J. Climate, 25, 6215–6232, http://dx.doi. org/10.1175/JCLI-D-11-00648.1, 2012.

Rotstayn, L., Collier, M., Dix, M., Feng, Y., Gordon, H., O\\\'Farrell, S., Smith, I. and Syktus, J. (2010). Improved simulation of Australian climate and ENSO-related climate variability in a GCM with an interactive aerosol treatment. Int. J. Climatology, vol 30(7), pp1067-1088, DOI 10.1002/joc.1952

The HadGEM2 Development Team: Martin, G. M., & 51 co-authors(2011)The HadGEM2 family of Met Office Unified Model Climate configurations, Geosci. Model Dev. 4, 723-757, doi:10.5194/gmd-4-723-2011.

Walters et al (2011). The Met Office Unified Model Global Atmosphere 3.0/3.1 and JULES Global Land 3.0/3.1 configurations Geosce Model Dev., 4, 1213-1271 doi10.194/gmdd-4-12-1213-2011

Webster, S., Brown, A.R., Cameron, D.R. and Jones, C.P. (2003). Improving the representation of orography in the Met Office Unified Model. Q.J.R. Meteorol. Soc.,129, 1989-2010.

Wu, TW., Song, LC., Li, WP., Wang, ZZ., Zhang, H., Xin, XG., Zhang, YW., ; Zhang, L., Li, JL., Wu, FH., Liu, YM., Zhang, F., Shi, XL., Chu, M., Zhang, J., Fang, YJ., Wang, F., Lu, YX., Liu, XW., Wei, M. Liu, QX., Zhou, WY., Dong, M., Zhao, QG., Ji, JJ., Li, L., Zhou, MY. (2014). An Overview of BCC Climate System Model Development and Application for Climate Change Studies. JOURNAL OF METEOROLOGICAL RESEARCH, Volume: 28,Issue1,pages 34-56.